

Optimization of quantum noise by completing the square of multiple interferometer outputs in quantum locking for gravitational wave detectors

Rika Yamada^a, Yutaro Enomoto^b, Atsushi Nishizawa^c, Koji Nagano^d, Sachiko Kuroyanagi^a, Keiko Kokeyama^d, Kentaro Komori^e, Yuta Michimura^b, Takeo Naito^a, Izumi Watanabe^a, Taigen Morimoto^a, Masaki Ando^b, Akira Furusawa^f, Seiji Kawamura^a

^a*Department of Physics, Nagoya University, Furo-cho, Chikusa-ku, Nagoya, Aichi 464-8602, Japan*

^b*Department of Physics, University of Tokyo, Bunkyo, Tokyo 113-0033, Japan*

^c*Research Center for the Early Universe (RESCEU), School of Science, The University of Tokyo, Tokyo 113-0033, Japan*

^d*Institute for Cosmic Ray Research, The University of Tokyo, 5-1-5 Kashiwa-no-Ha, Kashiwa, Chiba 277-8582, Japan*

^e*LIGO Laboratory, Massachusetts Institute of Technology, Cambridge, Massachusetts 02139, USA*

^f*Department of Applied Physics, School of Engineering, The University of Tokyo, 7-3-1 Hongo, Bunkyo-ku, Tokyo 113-8656, Japan*

Abstract

The quantum locking technique, which uses additional short low-loss sub-cavities, is effective in reducing quantum noise in space gravitational wave antenna DECIGO. However, the quantum noise of the main interferometer depends on the control systems in the sub-cavities. Here we demonstrate a new method to optimize the quantum noise independently of the feedback gain by completing the square in the quantum locking system. We successfully demonstrate in simulations that this method is effective in optimizing the homodyne angle to the best quantum-noise-limited sensitivity.

Keywords: Gravitational wave, DECIGO, quantum locking, squeezing, completing the square, Fabry-Perot cavity

1. Introduction

Gravitational wave was detected for the first time by LIGO in 2015 [1]. Many detections of gravitational wave from binary black holes and binary neutron stars have followed since [2]. Now, one of the next major targets is the primordial gravitational wave, which is believed to be produced during the inflation period [3]. Given that gravitational wave detection is the only observable direct proof of the inflation, its significance cannot be overstated. The decihertz interferometer gravitational wave observatory (DECIGO) is a Japanese future space mission, of which the primary goal is to detect the primordial gravitational wave [4]. It is a fleet of three drag-free spacecraft 1,000 km apart from one another.

In interferometric gravitational wave detectors, quantum noise is one of the most fundamental noises that limit their sensitivity [5]. To reduce quantum noise, squeezed light is often used in ground-based detectors [6]. However, the arms of DECIGO are 1,000 km long and optical loss due to diffraction would be too large (22 %) to use squeezed light. Instead, the quantum locking technique [7, 8, 9] could be employed in DECIGO, which is another effective technique in reducing quantum noise, utilizing short low-loss cavities.

To use the quantum locking, short sub-cavities are required to be implemented on the outer sides of the main cavity's mirrors. To lock the main mirrors to the sub-cavities yields reduction of the radiation pressure noise of the main mirrors, providing that the sub-cavities are operated with a lower laser-power than the main cavities. In addition, the radiation pressure noise of the main mirrors can be also eliminated at a certain frequency. To achieve it, homodyne detection must be implemented properly in the sub-cavities. Also, the homodyne angle of homodyne detection should be optimized for the particular frequency determined on the basis of each target science, which is possible only with precise estimation of the quantum noise as a function of the homodyne angle. The main problem is, however, that the quantum noise of the main interferometer depends on the control systems in the sub-cavities [10] because the control systems impose the sub-cavity's quantum noise to the main cavity's mirrors. Therefore, it is vital to develop a method to estimate the quantum noise independently of the control systems.

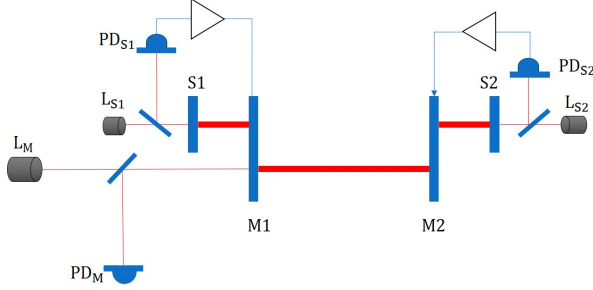


Figure 1: Basic configuration of the quantum locking. A main cavity consisting of two mirrors (M1, M2) is illuminated by a laser (L_M) and the reflected light is detected by a photodetector (P_{D_M}). Two sub-cavities consisting of the shared mirrors (M1, M2) and additional mirrors (S1, S2) are illuminated by two lasers (L_{S1} , L_{S2}) and the reflected lights are detected by the two respective photodetectors ($P_{D_{S1}}$, $P_{D_{S2}}$).

In this paper, we show a new method for it in which the best combination of outputs from main- and sub-cavities are taken into account. We then demonstrate that the best homodyne angle for the quantum noise can be determined with this method.

2. Theory

Figure 1 illustrates the basic configuration of the quantum locking; the sub-cavities are implemented on the outer sides of the main cavity's mirrors. The two mirrors of the main mirrors are shared by each cavity. Each sub-cavity is locked on resonance by controlling the corresponding main mirror.

Figure 2 shows a phaser diagram at the sub-cavity detection port. When laser light enters a sub-cavity, the phase fluctuation of the light is further affected with vacuum quantum fluctuations: a_1 and a_2 . When the laser light hits one of the mirrors in the sub-cavity, the mirror is physically shaken by an amount of amplitude a_1 in the form of quantum fluctuation. As a result, the phase fluctuation of the reflection light, so-called the radiation pressure noise (P_{M1} and P_{S1} for mirrors M1 and S1, respectively), is introduced.

Homodyne detection is a method to detect different quadratures. We use local light, which has the same frequency as the carrier light but a different phase in the homodyne detection. If we use the local light that rotates the phase of the sum of the carrier and local lights by η from that of the carrier, we can detect signals projected on the dashed line in Fig. 2. With this method, we can adjust the parameters so that the phase fluctuation of the S1 mirror (P_{S1}) and the $a1$ noise cancel each other at the detection output at a certain frequency. This means that we detect the phase fluctuation of the M1 mirror (P_{M1}) only. If we feedback the detected signals of the sub-cavities to the main cavity mirrors, we can completely eliminate the radiation pressure noise in the main cavity at a certain frequency for a given homodyne angle.

At high frequencies, however, the main cavity's quantum noise increases because the control system adds the sub-cavity's noise a_1 to the main cavity's mirror. At low frequencies, the quantum noise depends on to what extent the radiation pressure noise of the main cavity is replaced by that of the sub-cavity. As such, the quantum noise of the main cavity depends on the control system.

The best estimate of the quantum noise that is independent of the control system can be made by taking the best combination of the main cavity's output and the sub-cavities' outputs. Here, we obtain the best combination by completing the square.

Figure 3 is a schematic block diagram, which shows three cavities of the quantum locking. Each cavity has one detection port (V_m , V_{S1} , V_{S2}), and two quantum noise inputs: the amplitude quadratures (a_1, a_3, a_5) and the phase quadratures (a_2, a_4, a_6). Note that a_1, a_2 are redefined. Also, note that the main and sub-cavities are assumed to have end mirrors with 100 % reflectivity; no additional quantum fluctuations enter from the end mirrors. This assumption

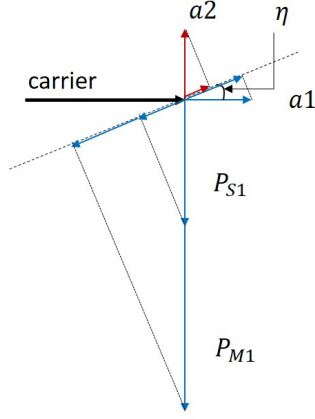


Figure 2: Phaser diagram at the detection port of a sub-cavity. “Carrier” indicates the laser carrier of the sub-cavity. a_1 is the amplitude quantum fluctuation and a_2 is the phase quantum fluctuation. P_{S1} and P_{M1} are the phase fluctuations of the reflected light caused by the motion of the mirrors, which is shaken by amplitude quantum fluctuation. η is the homodyne angle of the homodyne detection. Projected signals along the homodyne axis are also shown.

is used to demonstrate the effectiveness of the optimization method without any complications. Gravitational wave signals enter only the main cavity and they do not enter the other cavities because the sub-cavities are too small to be affected by gravitational waves. The outputs are given by Eqs.(1)-(3):

$$V_m = s + Aa_1 + Ba_2 + Ca_3 + Da_4 + Ea_5 + Fa_6 \quad (1)$$

$$Vs1 = Ga_1 + Ha_2 + Ia_3 + Ja_4 \quad (2)$$

$$Vs2 = Ka_1 + La_2 + Ma_5 + Na_6. \quad (3)$$

The parameters A to N are the coefficients of each noise source. Note that A to F are normalized so that the coefficient of s is unity in V_m . The parameters V_{s1} and V_{s2} are symmetric: $G = K$, $H = L$, $I = M$ and $J = N$. Let us introduce the combined output V with a coefficient χ , as defined in Eq.(4):

$$V = V_m + \chi (V_{s1} + V_{s2}). \quad (4)$$

Since all the parameters of a_1 to a_6 are independent of one another, we take the quadrature sum x^2 of the signal and all noises as follows (Eq.(5)):

$$x^2 = s^2 + \left\{ (|2G|^2 + |2H|^2 + 2|I|^2 + 2|J|^2) \left(\chi + \frac{2(AG^* + BH^* + CI^* + DJ^*)}{(|2G|^2 + |2H|^2 + 2|I|^2 + 2|J|^2)} \right) \left(\chi^* + \frac{2(A^*G + B^*H + C^*I + D^*J)}{(|2G|^2 + |2H|^2 + 2|I|^2 + 2|J|^2)} \right) \right\} \\ + \left\{ -\frac{4|AG^* + BH^* + CI^* + DJ^*|^2}{(|2G|^2 + |2H|^2 + 2|I|^2 + 2|J|^2)} + (|A|^2 + |B|^2 + |C|^2 + |D|^2 + |E|^2 + |F|^2) \right\}. \quad (5)$$

Here, if we choose χ in such a way that the second term of x^2 is 0, x^2 takes the smallest value and accordingly the third term is the minimum value of x^2 . Therefore, the square root of the third term is the minimum total noise normalized in terms of gravitational wave signals.

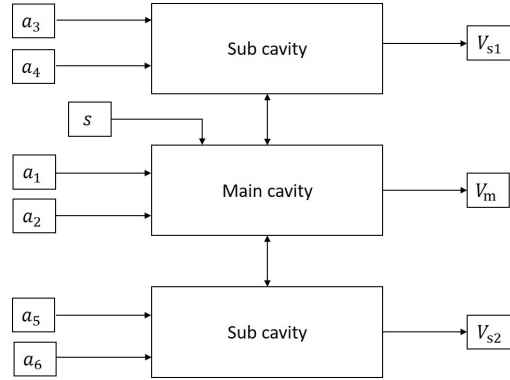


Figure 3: Schematic block diagram of the quantum locking. There are three cavities: a main and two sub-cavities. a_1, a_3 , and a_5 are the amplitude quantum fluctuations. a_2, a_4 , and a_6 are the phase quantum fluctuations. V_m, V_{s1} , and V_{s2} are the signals at the detection ports. S is the input (gravitational wave) signal.

3. Simulations

3.1. Simulation model

Following the previous section, where we have optimized the total noise of the main and sub-cavities, using the completing-square method, we here determine the best homodyne angle for our target frequency.

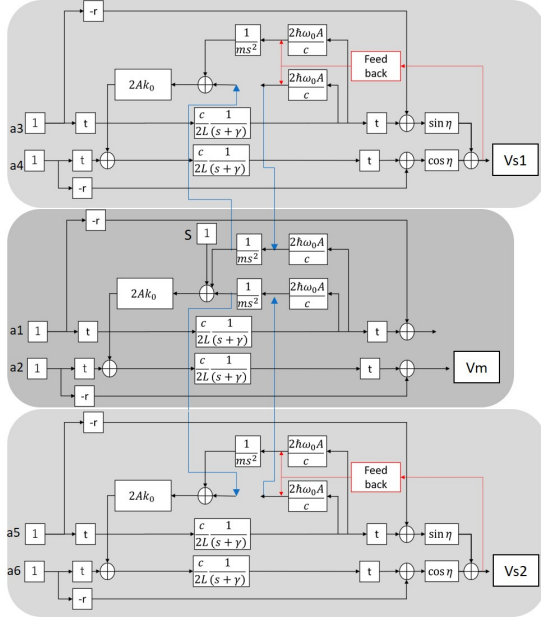


Figure 4: Detailed block diagram of the main cavity and the two sub-cavities. The quantum fluctuation a_1 is divided into transmission and reflection by t and r blocks. In the $c/2L(s + \gamma)$ block, the transmission is affected by the cavity pole inside the cavity. The $2\hbar\omega_0 A_0/c$ block combines the vacuum quantum fluctuation with the carrier light, producing force applied to the mirrors. The $1/ms^2$ block changes the force to the mirror displacement, which then produces a phase quantum fluctuation by $2A_0k_0$. It is added to the phase noise. The phase noise is affected by the cavity pole again. Homodyne detection is performed in the $\sin \eta$ and $\cos \eta$ blocks. Finally it is detected at V_m . Since the mirrors of the main cavity are shared with the sub-cavities, the $1/ms^2$ blocks are also shared. The feedback signal is added as a force to push a mirror in the sub-cavity.

Figure.4 shows a block diagram (similar to but more detailed than Fig. 3) that demonstrates a procedure to obtain the coefficients A to J in Eq.(1)-(3) (see also [11]). The center part is the main cavity. Quantum fluctuations (a_1 and a_2) are divided into the transmission and reflection by the input mirror of the main cavity with an amplitude transmissivity (t) and amplitude reflectivity (r) of the mirror. The mirror is assumed to have no optical loss: $t^2 + r^2 = 1$. The fluctuations are low-pass-filtered inside the cavity in the form of $c/2L(s + \gamma)$, where s is a Laplace complex variable and γ is the cavity pole. Note that we consider the case where each cavity is over-coupled. Specifically, γ is given by,

$$\gamma = \frac{\pi c}{2L\mathcal{F}} \quad (6)$$

$$\mathcal{F} = \frac{\pi\sqrt{r}}{1-r}, \quad (7)$$

where c is the speed of light, L is the arm length of the cavity, and \mathcal{F} is the finesse of the cavity. The amplitude quantum fluctuation is coupled with the carrier light, $2\hbar\omega_0 A_0/c$, where \hbar is the reduced Planck constant, ω_0 is the angular frequency of the light $\omega_0 = \frac{2\pi c}{\lambda}$, and A_0 is the amplitude of light $A_0 = \sqrt{\frac{2I_{in}}{\omega_0 \hbar}}$, which is a function of the intensity (I_{in}) of the light.

This force shakes the cavity mirrors: $1/ms^2$, where m is the mass of the mirror. The mirror motion causes a phase fluctuations of $2A_0k_0$, where k_0 is the wavenumber ($k_0 = \omega_0/c$).

When an output signal is detected with a conventional detection method, it is only a phase quadrature. Thus, V_m is the signal of the main cavity, if the feedback block of the main cavity is ignored for simplicity. The gravitational wave signal enters the block as a differential displacement of the mirrors.

The sub-cavities are basically the same as the main cavity. In the quantum locking, the mirrors of the main cavity are shared by the sub-cavities. We detect the output signals (V_{s1} and V_{s2}) of the sub-cavities, and feedback them to the mirror motion. Homodyne detection is performed with $\sin \eta$ and $\cos \eta$, where η is the homodyne angle.

In our simulations, we use optical and mechanical parameters on the basis of the pre-conceptual design parameters of DECIGO listed in table 1. The sub cavities' parameters are shown in table 2.

Table 1: Pre-conceptual design parameters of the main cavity of DECIGO

Cavity length	L	1000 km
Finesse	\mathcal{F}	10
Laser Power	P	100 W
Laser wavelength	λ	515 nm
Mirror mass	M	100 kg

Table 2: Parameters of the sub-cavities

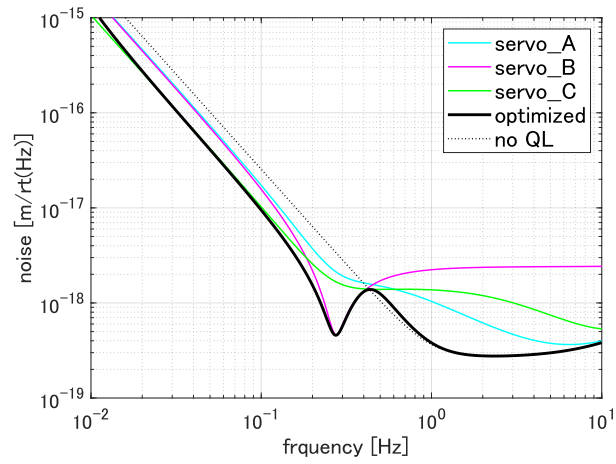
Cavity length	L	1 m
Finesse	\mathcal{F}	10
Laser Power	P	100 W
Laser wavelength	λ	515 nm
Mirror mass	M	100 kg

Though the laser power is 10 W in the pre-conceptual design of DECIGO, 100 W is used in our simulations because shot noise is reduced with the latter and hence it enables us to demonstrate the effect of the quantum locking more clearly.

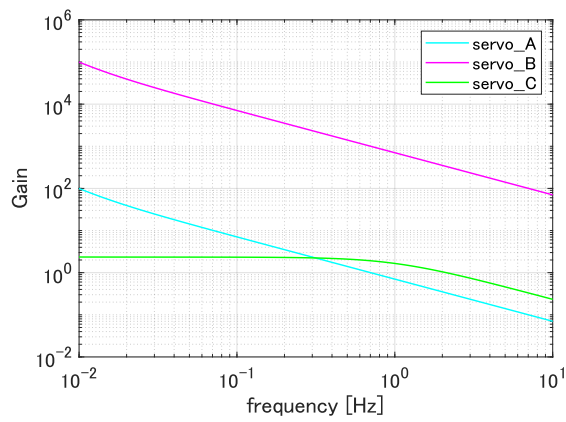
3.2. Optimization of quantum noise

Using our optimizing method (section 2) and model (section 3.1), we optimize the quantum noise in the system with the quantum locking. We calculate the noise with several feedback-loop gains and show it in Fig.5b. Servo A has a moderate gain at low frequencies, servo B has a high gain at high frequencies and servo C has a gain slightly higher than the unity at low frequencies. If we use the output of only the main cavity, the total quantum noise depends on the feedback gain (see servos A to C in Fig.5a). With servo A, the noise is lower at high frequencies, but the noise reduction at the best part is limited. With servo B, we achieve the best noise reduction at ~ 0.3 Hz. However, the noise is higher at most other frequencies. With servo C, the noise is lowest among the three servos at low frequencies. By contrast, the optimized total quantum noise with the completing-square method shows remarkable overall improvement (Fig.5a); it is as low as that given by servo A at high frequencies, as low as that by servo B at the middle and best frequency (~ 0.3 Hz), and as low as that by servo C at low frequencies. The optimized noise is the same even if the feedback of the sub cavity is turned off.

Figure 6 shows the noise budget of the optimized total noise. Noise a_{2_caused} limits the total noise at high frequencies only. At the middle and best frequency, noises a_{1_caused} and $a_{3,5_caused}$ show significant improvement, whereas the improvement in noises a_{2_caused} and $a_{4,6_caused}$ is limited. At low frequencies, noises a_{1_caused} and $a_{3,5_caused}$ limit the total noise.



(a)



(b)

Figure 5: (a) Total quantum noise of the system. Bold black line shows the total noise, which is optimized with the completing-square method. Colored solid lines show the quantum noise at the output of the main cavity with three variations of the servo system: servos A, B, and C. Dotted line (“no QL”) shows the total noise without the quantum locking. (b) Loop gains of the three servo systems of the sub-cavities as examples.

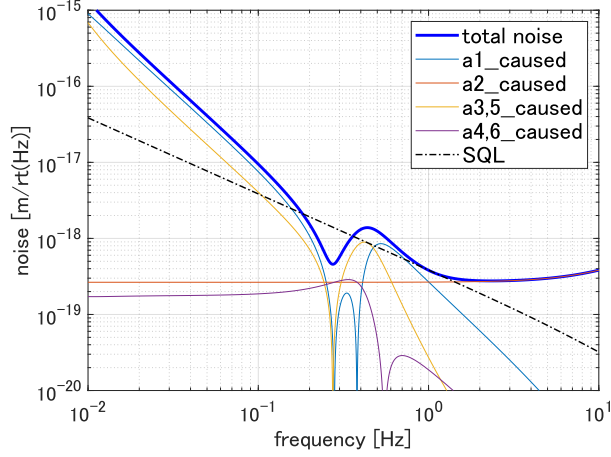


Figure 6: Noise components of the optimized total quantum noise. The total noise is the sum of a_{1_caused} to a_{6_caused} noises. “SQL” is the standard quantum limit.

3.3. Signal to noise ratio

We search for the best homodyne angle on the basis of the optimized total noise. We evaluate the total noise level in the form of the signal-to-noise ratio (SNR) [5] for the primordial gravitational wave, according to Eq(8):

$$SNR = \frac{3H_0^2}{10\pi^2} \sqrt{T} \left[\int_{0.1}^1 df \frac{2\gamma(f)^2 \Omega_{GW}^2(f)}{f^6 P_1(f) P_2(f)} \right]^{1/2}. \quad (8)$$

Table 3: Parameters used to estimate the SNR

H_0	Hubble parameter	$70 \text{ km} \cdot \text{sec}^{-1} \cdot \text{Mpc}^{-1}$
T	time for correlation	3 years
f	frequency	0.1 to 1 Hz
γ	correlation function	1
Ω_{GW}	energy density	10^{-16}
P_1, P_2	noise power spectral densities	optimized in Figure 5

P_1 and P_2 are the total noises, which are calculated in section 3.2. Here we assume them to be equal to each other. T is the observation time, and is set to 3 years, as DECIGO plans to take a 3-years correlation. Ω_{GW} is the energy density upper limit of the primordial gravitational wave in the standard inflation model [12, 13]. The target frequency band is chosen to be 0.1 to 1 Hz because confusion limiting noise is significant below 0.1 Hz, which is caused by inseparable gravitational waves coming from binaries of white dwarfs etc. in our galaxy. This means that we cannot detect the primordial gravitational wave at frequencies lower than 0.1 Hz. Table 3 summarizes these parameters. In consequence, the SNR at the output of only the main cavity without the sub-cavities is calculated to be 1.41.

Figure 7 shows the SNR dependence on the homodyne angle. With the completing-square method, the best SNR in the frequency band from 0.1 to 1 Hz is 33.2 with the best homodyne phase. This is 23.5 times better than the original noise that is obtained without the quantum locking. It should be noted that in the above estimation only the quantum noise is considered. In reality, some other noises are also expected to limit the sensitivity. Thus, the realistic best homodyne angle could be different.

4. Conclusions

We invented the method to optimize the quantum noise independent of feedback gain. Completing the square of multiple interferometer outputs is the key technology. We demonstrated that this method is highly effective, for

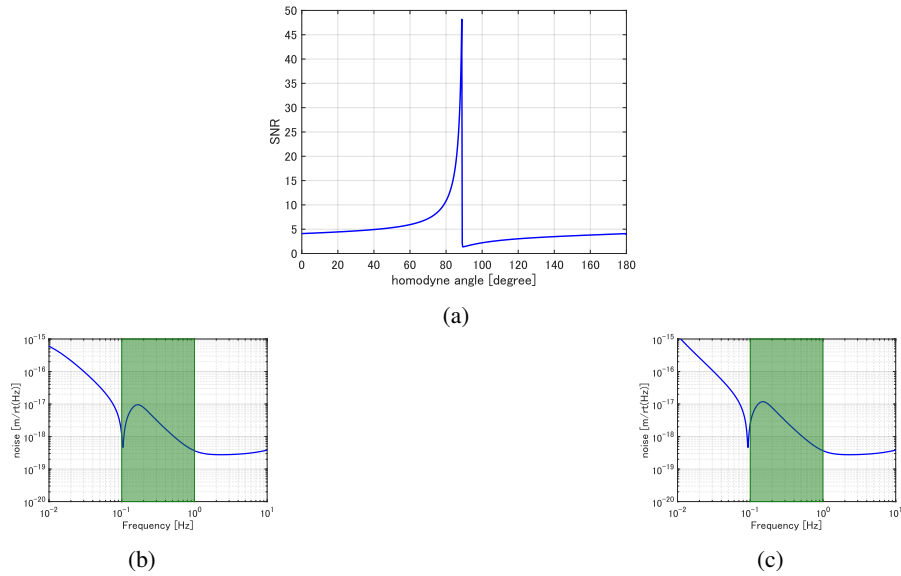


Figure 7: (a) Homodyne phase dependence on the SNR. (b) the total noise curve with a homodyne phase corresponding to the peak of the SNR in Panel (a). (c) the total noise with a homodyne phase corresponding to the lowest SNR in Panel (a).

example, in optimizing the homodyne phase to the best quantum-noise-limited sensitivity. This method can be used in general cases to optimize the quantum noise when there are two or more outputs in the system.

Acknowledgments

We would like to thank Masayuki Nakano for helpful discussion. This work was supported by Daiko Foundation and JSPS KAKENHI Grant Number JP19H01924.

References

- [1] B. P. Abbott et al, "Observation of Gravitational Waves from a Binary Black Hole Merger", *Phys. Rev. Lett.* 116 (2016) 061102. doi: <https://doi.org/10.1103/PhysRevLett.116.061102>
- [2] B. P. Abbott et al, "GWTC-1: A Gravitational-Wave Transient Catalog of Compact Binary Mergers Observed by LIGO and Virgo during the First and Second Observing Runs", *Phys. Rev. X.* 9 (2019) 031040. doi: <https://doi.org/10.1103/PhysRevX.9.031040>
- [3] Michele Maggiore, "Gravitational Wave Experiments and Early Universe Cosmology", *Phys. Rept.* 331 283-367. doi: [https://doi.org/10.1016/S0370-1573\(99\)00102-7](https://doi.org/10.1016/S0370-1573(99)00102-7)
- [4] N. Seto, S. Kawamura, and T. Nakamura, "Possibility of Direct Measurement of the Acceleration of the Universe Using 0.1 Hz Band Laser Interferometer Gravitational Wave Antenna in Space", *Phys. Rev. Lett.* 87 (2001) 221103. doi: <https://doi.org/10.1103/PhysRevLett.87.221103>
- [5] V. B. Braginsky and F. Ya. Khalili, "Quantum nondemolition measurements: the route from toys to tools", *Rev. Mod. Phys.* 68 (1996) 1-11. doi: <https://doi.org/10.1103/RevModPhys.68.1>
- [6] Lisa Barsotti and Jan Harms and Roman Schnabel, "Squeezed vacuum states of light for gravitational wave detectors", *Report on Progress in Physics* 82 (2018) 016905. doi: 10.1088/1361-6633/aab906
- [7] S.Kawamura, O.Miyakawa and K.Somiya, "Reduction of Radiation Pressure Noise Using an Auxiliary Interferometer in a Laser Interferometric Gravitational Wave Antenna", submitted to *Appl.Opt.* 2001
- [8] Jean-Michel Courty, A. Heidmann, M. Pinard, "Quantum locking of mirrors in interferometers", *Phys. Rev. Lett.* 90 (2003) 083601. doi: <https://doi.org/10.1103/PhysRevLett.90.083601>
- [9] A Heidmann, J.-M. Courty, M. Pinard, J. Lebars, "Beating quantum limits in interferometers with quantum locking of mirrors", *J.Opt.B Quant.Semiclass.Opt.* 6 (2004) S684. doi: 10.1088/1464-4266/6/8/009
- [10] Hidehiro Yonezawa, Takao Aoki, Akira Furusawa, "Demonstration of quantum teleportation network for continuous variables", *Nature* Vol.431 No.7007 (2004)
- [11] Yutaro Enomoto, Master thesis (2017)
- [12] Planck Collaboration, "Planck 2018 results. X. Constraints on inflation", *Astro-ph.CO arXiv preprint arXiv:1807.06211*, 2018.
- [13] Sachiko Kuroyanagi, Shinji Tsujikawa, Takeshi Chiba, Naoshi Sugiyama, "Implications of the B-mode Polarization Measurement for Direct Detection of Inflationary Gravitational Waves", *PhysRevD.* 90 (2014) 063513. doi: <https://doi.org/10.1103/PhysRevD.90.063513>